Redox Reactivity of Colloidal Nanoceria and Use of Optical Spectra as an *In-Situ* Monitor of Ce Oxidation States

*Delina Damatov, Stephanie M. Laga, Elizabeth A. Mader, Jing Peng, Rishi G. Agarwal, and James M. Mayer**

Department of Chemistry, Yale University, New Haven, CT 06520-8107, USA
E-mail: james.mayer@yale.edu

KEYWORDS. Cerium oxide nanocrystals, Ce oxidation states, chemical reactivity, UV-visible absorbance, X-ray absorption spectroscopy (XAS).

ABSTRACT. Nanoscale cerium oxide is of increasing interest in catalysis, biomedicine, renewable energy and many other fields. Its versatility derives from the ability to form non-stoichiometric oxides that include both Ce^{3+} and Ce^{4+} ions. This work describes oxidation and reduction reactivity of colloidal cerium oxide nanocrystals, termed nanoceria, under very mild solution conditions. For instance, the as-prepared nanoceria oxidizes hydroquinone to benzoquinone, with reduction of some of the Ce^{4+} ions. Highly reduced nanoceria, prepared by UV irradiation in the presence of ethanol, oxidize hydroquinone back to benzoquinone. This and related reactivity allow tuning of the average cerium oxidation state in the nanocrystals without

changes in size or other properties. The amounts of Ce^{3+} and Ce^{4+} in the nanoceria were determined both by X-ray absorption spectroscopy and from the stoichiometry of the reactions, measured using ^{1}H NMR spectroscopy. The results demonstrate, for the first time, that the optical absorbance of nanoceria is linearly related to the percent Ce^{3+} in the sample. The decrease in absorption (blue-shift of the band edge) is due to increasing amounts of Ce^{3+}, not to a quantum confinement effect. These findings demonstrate the facile solution reactivity of nanoceria and establish UV-visible spectroscopy as a powerful new tool for *in situ* determination of Ce oxidation states in ceria nanomaterials.

INTRODUCTION

Cerium oxide (ceria) is a highly versatile material used in applications ranging from solid oxide fuel cells to protective coatings, antioxidant agents, solar cells, optical films, gas sensors and polishing powders.[1] Ceria is a non-stoichiometric oxide that is typically characterized as having oxygen atoms missing from the lattice (O vacancies) with corresponding reduced Ce atoms. This phenomenon becomes especially important for nanoscale materials. Therefore, the formula for cerium oxide nanoparticles is often written as CeO_{2-x}, where x ranges from 0 to 0.5.

Perhaps the largest impact of ceria-based materials has been in redox catalysis, due to the ability of the cerium ions to switch between Ce^{3+} and Ce^{4+} oxidation states.[2, 3] Reduction of cerium oxide is possible either by creation of oxygen vacancies (the traditional approach)[4, 5] or by adsorption of a hydrogen atom.[6, 7] H-atom adsorption usually proceeds at elevated temperatures (400-700 K) under H_2 atmosphere, forming both surface[8, 9] and interstitial[10, 11] hydroxyls upon reduction. Recent studies suggest that hydroxyls on ceria are formed in parallel to oxygen vacancies[12] and play a crucial role in ceria reducibility and reactivity.[13] While these

redox processes have been studied extensively for high-temperature solid-gas phase reactions[14] and for thin films,[15] they have been much less explored for colloidal suspensions of cerium oxide nanocrystals (NCs, nanoceria).

The redox reactivity of colloidal nanoceria has been studied mostly in aqueous suspensions in the context of biomedical applications and its environmental impact.[16-18] The ability of nanoceria to be an *in vivo* antioxidant has been examined, including its quenching of reactive oxygen species (ROS), cell protection against oxidative stress, and toxicity of nanoceria.[19-22] Nanoceria also reacts with biologically relevant reducing agents such as ascorbate and catechols like dopamine.[23, 24] These studies have shown reduction of Ce^{4+} and frequent ligand binding to the nanocrystal surface. For some individual substrates, the optical spectra can be part of a valuable analytical method. However, there have been few detailed studies of the reactions of nanoceria that quantitatively correlate the stoichiometry and spectroscopy of these materials, using a fundamental rather than application-oriented perspective.

In parallel with these studies of nanoceria, there has been significant development of the molecular chemistry of cerium. These areas are starting to intersect, most notably in recently reported large cerium-oxide-carboxylate clusters.[25] These clusters show the stoichiometry, coordination sphere, and locations of oxygen vacancies for ceria and thus can be viewed as atomically precise ceria nanoparticles. Related smaller clusters have also been described.[26] In more traditional cerium coordination chemistry with multidentate ligands, recent studies have demonstrated that the Ce^{4+}/Ce^{3+} reduction potential varies substantially with the nature of the ligand sphere.[27-30] These ligand effects are likely relevant to the distribution of Ce^{3+} vs. Ce^{4+} in the distinct sites within the oxide-carboxylate clusters, and perhaps in the nanoceria as well. The

coordination chemistry also provides some insights into the broad range of redox reactivity of the nanoceria that is described below.

For ceria materials, the direct determination of the average Ce oxidation state is an essential part of characterization. The most common way to measure Ce^{3+}/Ce^{4+} ratios is by X-ray Photoelectron Spectroscopy (XPS). However, this *ex-situ* high vacuum method was shown to induce reduction of the sample during the measurement,[31, 32] resulting in substantially higher values of Ce^{3+}. Alternative techniques include Energy Loss Near Edge Structure (ELNES)[33] analysis by TEM and X-ray Absorption Near Edge Structure (XANES)[34] analysis by synchrotron irradiation, although neither is easily accessible.

The optical spectrum of cerium oxide is characterized by a strong absorption edge in the near UV-visible region, typical for a wide gap metal oxide semiconductor.[35] For nanoceria, the edge is very broad and its position is sensitive to physical and chemical modifications of the NC, for instance, blue-shifting with decreasing NC size.[36-38] Some researchers relate the shift of the absorption edge to changes in Ce^{3+}/Ce^{4+} ratio,[39, 40] while others refer to quantum confinement effects.[41, 42] Since a decrease in CeO_{2-x} NC size is also accompanied by an increase in Ce^{3+} content,[43-45] these two effects are often convolved when analyzing their contribution to the position of the absorption band.

The work reported here systematically and quantitatively connects ceria NC redox reactivity to optical spectroscopy. We describe new stoichiometric reactivity of nanoceria with well-defined molecular oxidants and reductants under very mild conditions, using reagents such as benzoquinone and hydroquinone in unreactive solvents such as cyclohexane and THF. The reaction progress and stoichiometry were monitored by UV-visible and ^1H NMR spectroscopies. X-ray absorption spectroscopy (XAS) was used to measure the Ce^{3+}/Ce^{4+} ratio directly. Good

mass balance was obtained between the change in the cerium oxidation state and the small molecule products in solution. The same optical spectra were obtained when the same Ce^{3+}/Ce^{4+} ratio was obtained with different reagents.

The results show that the optical transitions are not a result of reactant or product binding to the NCs. This contrasts with the prior aqueous studies, where the absorbance was directly related to ligand binding. The data demonstrate that the optical spectra respond only to the valence state of the ceria. The mild chemical reactions do not change the size of the NCs, so the changes in the optical spectra are not due to quantum confinement. The data show a *quantitative* correlation between the optical absorption and the percent Ce^{3+} in two different kinds of nanoceria. Therefore, the optical spectra of cerium oxide NCs can be used to monitor their Ce^{3+}/Ce^{4+} ratio. This correlation is a powerful tool for the study of these increasingly important nanomaterials.

EXPERIMENTAL SETUP

Complete experimental details and additional data are given in the Supporting Information (SI). Oleate-capped ceria NCs (**OLE-Ce**) were synthesized following a published procedure with minor modifications,[46] using sodium oleate, ceric ammonium nitrate and aqueous ammonia. After drying at 90 °C for 24 h under air, the NCs were suspended in cyclohexane, and stored under N_2 at -35 °C. Methoxyacetic acid–capped NCs (**MAA-Ce**) were obtained from Strem Chemicals. Cerium concentrations were determined using ICP-MS analysis. Photochemical reductions were performed with added alcohols under N_2 and UV irradiation.

Reactions of **OLE-Ce** were typically preformed as cyclohexane or cyclohexane/thf suspensions. Reactions were set up in the glove box and run in air-free optical cuvettes or NMR

tubes. Reactions of **MAA-Ce** were typically run in water or methanol. Products were identified and quantified by optical or ^{1}H NMR spectra and comparisons with authentic samples.

Fluorescence X-ray absorbance measurements at the Ce LIII-edge (5723 eV) were acquired at the Advanced Photon Source, Argonne National Laboratory. Sample manipulations in most cases were performed in an inert atmosphere glovebox. Data analysis followed literature procedures (see SI).

RESULTS AND DISCUSSION

I. General Methodology and Approach to Studying Ceria Reactivity and Spectroscopy. Two different types of ceria NCs were used for this study: oleate–capped cerium oxide (**OLE-Ce**), prepared by published methods,[46] and commercially available methoxyacetic acid–capped nanoceria (**MAA-Ce**). TEM and p-XRD revealed both materials to be crystalline, roughly spherical, and fairly monodispersed (**Figure 1**, Figures S1-S3). The **OLE-Ce** have an average diameter of 2.1 ± 0.2 nm, which corresponds to only about 4 unit cells across and ca. 140 Ce atoms per particle.[47] The **MAA-Ce** are slightly larger, 2.9 ± 0.3 nm, ca. 5-6 unit cells across and 350 Ce atoms per particle. **OLE-Ce** are lipophilic, soluble in non-polar organics, while **MAA-Ce** are soluble in water or polar solvents. Three independently made batches of **OLE-Ce** (-**a**, -**b**, and -**c**) were analyzed. Although quite similar in diameter (2.0 - 2.2 nm, Figure S2), they vary in their Ce^{3+}/Ce^{4+} ratio, as will be discussed below. All samples form clear colloidal solutions (Figure 1) that are suitable for optical absorption and NMR spectroscopic studies. The UV-visible spectra of the nanoceria have a strong and broad absorption edge below 400 nm. Previous studies used concentrated nanoceria solutions so that the spectrum was oversaturated below 400 nm, so the changes were observed as red and blue-shifts of the edge position.[48-50] In contrast, this work uses

dilute solutions of ceria NCs (≤0.25 mM in Ce ions), so that changes in the full absorption edge between 220 – 400 nm could be monitored during the course of chemical reactions. This small change provided important new insights, as the previously report blue shifts were found instead to be general decreases in absorbance (*vide infra*).

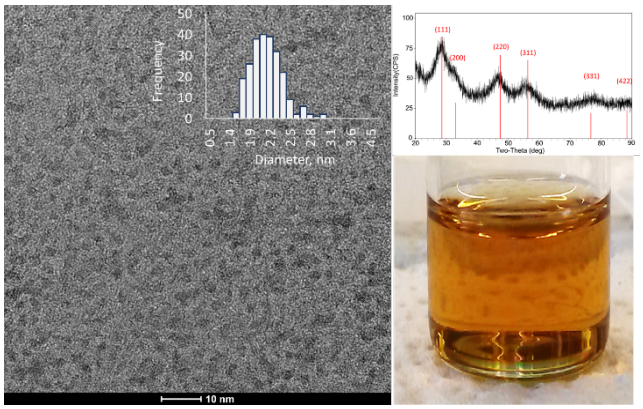

Figure 1. Ceria NCs used in this study. TEM image along with size histogram (left), p-XRD (right, top) and cyclohexane solution (right bottom) of **OLE-Ce**.

The general methodology used in this study was reacting colloidal solutions of ceria NCs with molecular redox reagents while following the changes by optical spectroscopy and 1H NMR. In parallel, the same reaction mixtures were subjected to XANES analysis to directly obtain the ratio of Ce oxidation states. Finally, all the techniques were correlated to connect between reactivity, absorbance spectra, and Ce oxidation states.

II. Chemical Reactions with Oxidants and Reductants Monitored by Optical and NMR Spectroscopies. 1,4-Hydroquinone (H_2Q) was chosen as the initial reagent to reduce nanoceria. As prepared **OLE-Ce** NCs in cyclohexane were titrated with different amounts of H_2Q (**Figure 2A**) and the optical spectra were monitored over the course of about 16 h. at r.t. The spectral

changes could be described as a blue-shift of the very broad, sloping absorption edge. However, they are more correctly described simply as a decrease in optical density (OD), since the absorbance decreases over the whole spectrum. The change in the ceria band edge absorbance was best observed at 340 nm, where the absorption of both H_2Q and the oxidized product, 1,4-benzoquinone (BQ), are negligible (Figure S4). As more H_2Q was added (0.1 to 1.0 molar equivalents to the number of Ce atoms), the OD_{340} decreased further until saturation behavior was observed (**Figure 2B**). The strong peak at 298 nm that grows in is due to the presence of excess unreacted H_2Q.

The final reaction mixture was analyzed by ^{1}H NMR to verify and quantify the product of oxidation, 1,4-benzoquinone (BQ, Figure S5). The oxidation of H_2Q to form BQ is a $2e^-/2H^+$ process, that must be accompanied by the reduction of Ce^{4+} to Ce^{3+} in the NCs to balance the stoichiometry. Using the number of equivalents of BQ produced in the reaction (determined by ^{1}H NMR), the optical density at 340 nm can be correlated with the extent of the NCs reduction.

In this case, and in every reaction we have examined, *there is a linear relationship between the OD_{340} and the number of electrons transferred to nanoceria* (**Figure 2C**). In total, upon addition of excess H_2Q, there was a formation of ca. 0.06 molar equivalents of BQ, that corresponds to reduction of 12% of the total Ce atoms.

An alternative way to reduce nanoceria is by UV irradiation in the presence of ethanol (EtOH). Photochemical reduction of semiconducting nanoparticles in the presence of a sacrificial reductant is well described in the literature.[51, 52] This procedure resulted in substantial reduction of the nanoceria, as was evidenced by even more pronounced decrease (blue-shift) of the absorption edge (**Figure 2D**). The OD at all the wavelengths between 220 – 400 nm declined with increasing irradiation time (from 15 min to 3 h), corresponding to increased extent of

reduction. More quantitative analysis of the changes in Ce oxidation states was obtained with XAS studies, as described below.

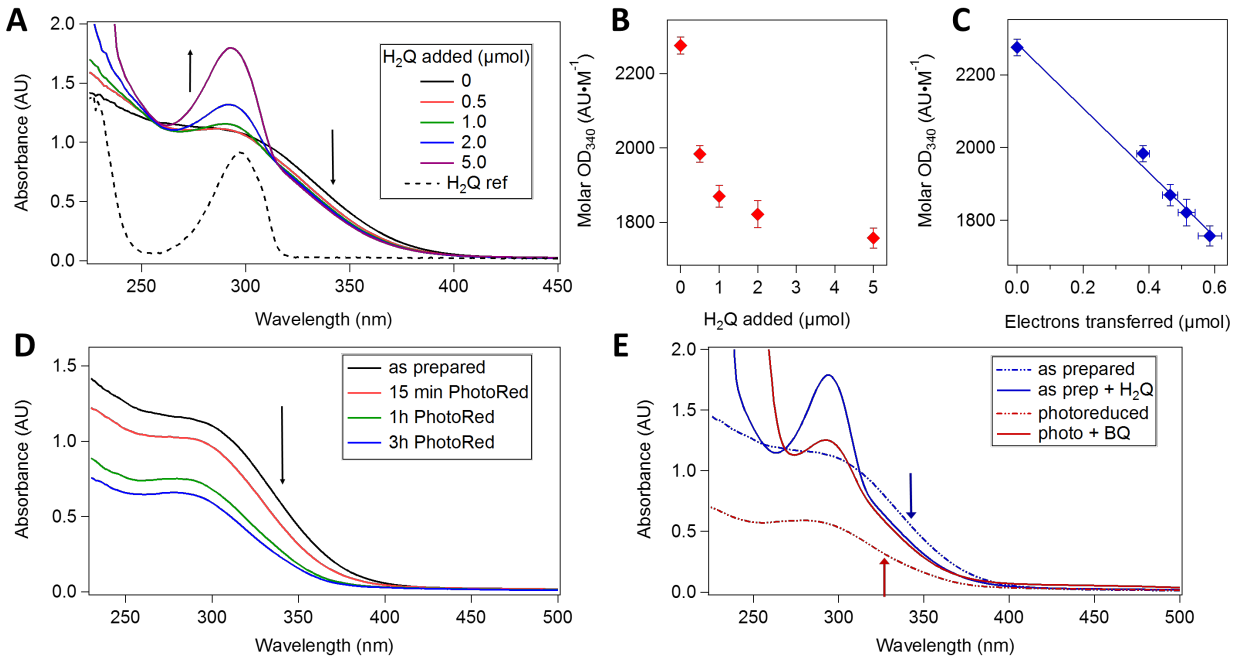

Figure 2. Changes in the optical absorption spectra of nanoceria as a result of redox processes. (A) Optical spectra of 5 μmol **OLE-Ce** (the total concentration of Ce ions) in cyclohexane/THF (2:1) upon addition of various amounts of H_2Q (0.5 – 5 μmol). The initial spectrum is shown in black. H_2Q (5 μmol) absorption spectrum is shown in the dashed line. (B) The molar absorbance of **OLE-Ce** at 340 nm after addition of different amounts of H_2Q. (C) The molar absorbance of **OLE-Ce** at 340 nm as a function of the number of electrons transferred to nanoceria (2 times the quantity of BQ formed by ^{1}H NMR). Errors are reported as the standard deviation of replicates or 10% of the median, whichever was greater. (D) Optical spectra of **OLE-Ce** after various irradiation times for the photochemical reduction with ethanol. The initial spectrum is shown in black. (E) Optical spectra of native (as-prepared) and photo-reduced **OLE-Ce** upon addition of H_2Q and BQ respectively (1 mol equiv). The initial spectra are shown as dotted lines.

The addition of BQ to the photochemically reduced **OLE-Ce** NCs is in essence the reverse of the reaction of as-prepared NCs with H_2Q described above. This reaction caused an *increase* in the optical absorbance (a red shift of the absorption edge), the reverse of the bleaching observed in the H_2Q reaction and upon photoreduction. Formation of the reduced product, H_2Q, was observed from the absorption peak at 298 nm (**Figure 2E**) and by ^{1}H NMR (Figure S6). The NMR spectra of these reactions generally showed good mass balance, with the sum of the benzoquinone and hydroquinone staying fairly constant over the reactions. There was no indication of either of these reagents binding significantly to the ceria, or loss of capping ligands during the reactions (Figure S19). This contrasts with prior studies using catechols, which are known to be much stronger ligands to oxophilic metal centers than the 1,4-substituted substrates used here.

Similar reactivity studies were performed with **MAA-Ce** and H_2Q, as well as with photochemically reduced **MAA-Ce** and BQ. The results paralleled those obtained with **OLE-Ce** samples (UV-visible, ^{1}H NMR, Figures S7-S9). The specific changes in the molar absorption were correlated with Ce oxidation states, measured by XAS (**Table 1** below).

Interconversion of H_2Q and BQ is not a pure electron transfer redox couple but rather involves $2e^-$ and $2H^+$. Thus, in some ways, these reactions resemble the net hydrogen atom transfer (HAT) or proton-coupled electron transfer (PCET) reactions of ZnO and TiO_2 nanocrystals that we have described previously.[53] Photoreduction by UV irradiation in the in the presence of ethanol also likely adds protons as well as electrons.[53]

Similar reactivity and spectroscopic changes were observed upon reaction of **OLE-Ce** NCs with other hydrogen atom donors and acceptors, showing the generality of the chemistry observed. 2,2,6,6-tetramethylpiperidin-1-yl-hydroxyl (TEMPOH) is an excellent H-atom donor

because of its weak O–H bond, forming the corresponding stable nitroxyl radical TEMPO. Addition of TEMPOH to the as-prepared NCs resulted in the decrease of the absorption band (reduction of Ce^{4+} to Ce^{3+}), while TEMPO oxidizes to the photo-reduced NCs with an increase in the optical density, Figure S10. Thus the $1e^{-}/1H^{+}$ TEMPOH/TEMPO• redox pair showed a similar reactivity to the $2e^{-}/2H^{+}$ H_2Q/BQ couple, consistent with their similar O–H bond dissociation free energies (BDFEs in DMSO, 68 kcal mol^{-1} for TEMPOH and 73 kcal mol^{-1} average for H_2Q/BQ, likely a little weaker in cyclohexane).[54] 2,4,6-tri-tert-butyl-phenol ($^{t}Bu_3PhOH$) did not reduce the as-prepared nanoceria, consistent with its higher BDFE of 81 kcal mol^{-1} in DMSO.[54] In the reverse direction, the stable phenoxyl radical $^{t}Bu_3PhO$• oxidized photo-reduced NCs with formation of the reduced phenol, $^{t}Bu_3PhOH$ (Figures S11-S12).

Similar spectroscopic changes were also observed upon oxidation of nanoceria with formal oxygen atom transfer reagents. Reactions of *tert*-butyl hydrogen peroxide (TBHP) with both as-prepared and photo-reduced samples of **OLE-Ce** showed a gradual increase in the OD (Figure S13A), as expected for an oxidation (TBHP does not absorb in this region). Both as-prepared and initially photo-reduced nanoceria yield essentially the same spectrum upon oxidation (the same Ce^{3+}/Ce^{4+} ratio) (Figure S13B). The reaction of iodosobenzene (PhIO) with **MAA-Ce** also showed an increase in absorbance, oxidation of Ce (by XAS, see below) and formation of the reduced product, iodobenzene (PhI, by ^{1}H NMR; Figures S14-S15).

The use of these *inner-sphere* redox reagents in inert solvents has strong advantages for the study of Ce oxidation states and optical spectra. The amount of redox change in the nanoceria was easily monitored through NMR spectra of the oxidized and reduced molecular products. A remarkably wide range of average cerium oxidation states is accessible, from 13% to 67% Ce^{3+}, without other substantial changes in the nature of the nanoceria (see below). This is possible

because the reagents donate or accept H-atoms or O-atoms, so that charge balance is maintained in the various reactions. The inner-sphere reactions of these NCs have parallels in the chemistry of cerium complexes,[30] and the wide range of redox agents used here is consistent with the range of reduction potentials reported for molecular compounds.[28,29] In contrast, the use of outer-sphere electron transfer reagents such as ferrocene/ferrocenium ($FeCp_2/FeCp_2^+$), would have resulted in substantial accumulation of positive or negative charge on the nanoceria, preventing such wide changes in cerium oxidations.

III. Cerium Oxidation States from X-ray Absorption Spectroscopy (XAS). To study the changes in oxidation states of the nanoceria, XAS experiments were done at the Advanced Photon Source (APS) at Argonne National Laboratory. *In situ* XANES were performed on reaction mixtures containing ceria NCs to determine the Ce^{3+}:Ce^{4+} ratio directly in solution. The ratio was determined by simulating the XANES spectra using a set of Gaussian and Arctan functions (**Figure 3A**), following a common procedure (see SI).[55-57]

The three distinct batches of **OLE-Ce** studied here (-**a**, -**b**, and –**c**), as synthesized, varied substantially in the fraction of Ce^{3+} therein. They ranged from 22% Ce^{3+} for **OLE-Ce-c** to 36% for the **OLE-Ce-b** sample. It is not clear what factor(s) in the synthesis procedure lead to these differences. The slightly larger average size of the (**-c**) batch (2.2 nm vs. 2.0 nm for (**-b**)) seems unlikely to be sufficient to explain this large difference in % Ce^{3+}.

XAS was used to determine the %Ce^{3+} in samples from a variety of chemical reactions, using all three of the batches of **OLE-Ce**, and using the **MAA-Ce** samples. The determined %Ce^{3+} values for the 24 different samples are listed in Table 1. The changes in the determined percentages of Ce^{3+} agreed with independent measurements from the amount of H_2Q, BQ, or

other molecular products formed in parallel solutions studies by ^{1}H NMR (Figure S16, Table S3).

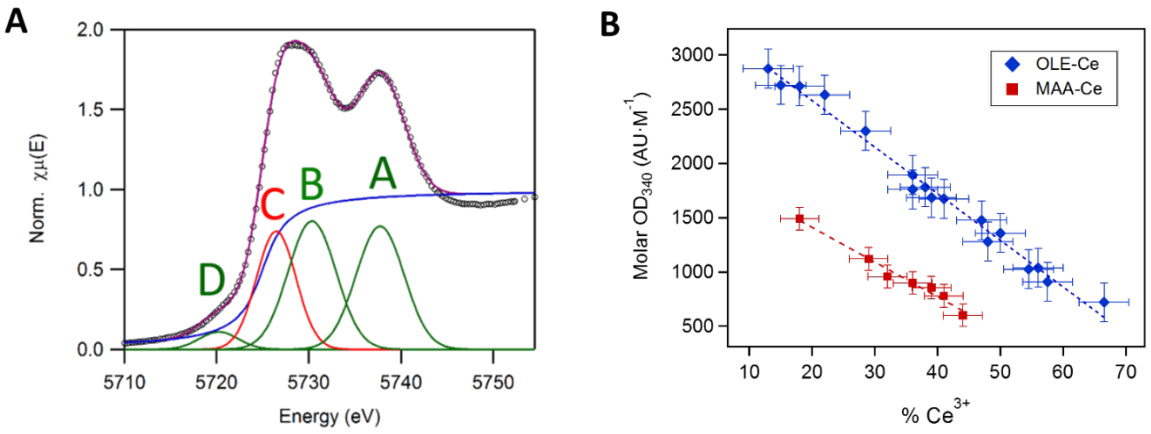

Figure 3. XANES analysis of cerium oxide NCs. (A) As-prepared **OLE-Ce** spectra (○) with component Arctan (blue (step = 1, width = 2, E0 = 5725 eV) and Gaussian functions (green/red) used to fit (purple) relative oxidation states. Peaks A-D correspond to the transitions in Table 1S. (B) Molar absorption dependency of nanoceria on % Ce^{3+} measured by XANES. Errors are given as the standard deviation from replicates or 10% of the median, whichever was greater.

Table 1. Ce oxidations states, chemical and photochemical reactions, and molar OD at 340 nm of various samples analyzed by XANES.

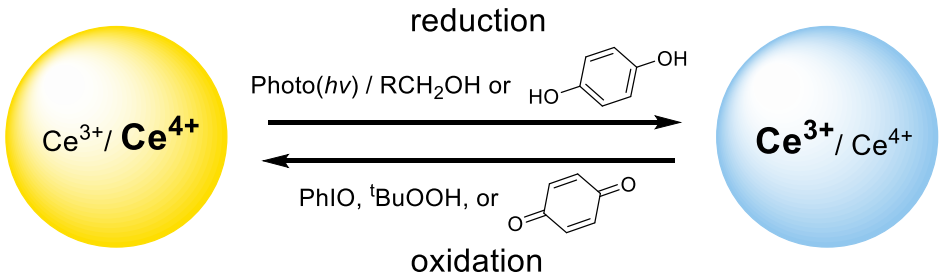

Sample	Molar OD_{340}	% Ce^{3+}	Sample	Molar OD_{340}	% Ce^{3+}
OLE-Ce-a[a]	2299	28.5	**OLE-Ce-b** – 1 h Photo[a,b]	721	66.5
OLE-Ce-b[a]	1894	36	**OLE-Ce-b –** H_2Q 1 mol/eq[c]	1357	50
OLE-Ce-c[a]	2631	22	**OLE-Ce-b –** H_2Q 0.1 mol/eq[c]	1476	47
OLE-Ce-a – ¼ h Photo[a,b]	1781	38	**OLE-Ce-b** – ^{t}BuOOH[a]	2711	18
OLE-Ce-a – 1 h Photo[a,b]	1025	54.5	**OLE-Ce-b –** 1 h Photo + BQ[b,c]	1280	48
OLE-Ce-a – 3 h Photo[a,b]	908	57.5	**MAA-Ce**[d]	956	32
OLE-Ce-a – H_2Q 1 mol/eq[c]	1761	36	**MAA-Ce** – 1 h Photo[d,e]	600	44
OLE-Ce-a – 1 h Photo + BQ[c]	1685	39	**MAA-Ce** – H_2Q[d]	780	41.5
OLE-Ce-a – ^{t}BuOOH[a]	2721	15	**MAA-Ce** – 1 h Photo + BQ[d,e]	856	39
OLE-Ce-a – 3 h Photo + BQ[b,c]	1672	41	**MAA-Ce** – PhIO[f]	1490	4
OLE-Ce-a – 3 h Photo + NMO[b,c]	1038	56	**MAA-Ce**[f]	1122	29
OLE-Ce-a – 3 h Photo + ^{t}BuOOH[a,b]	2874	13	**MAA-Ce** – H_2Q[f]	898	36

[a] Cyclohexane, N_2. [b] 4 mol/eq EtOH. [c] Cyclohexane/THF (2/1), N_2 [d] H_2O, N_2. [e] 4 mol/eq MeOH. [f] MeOH, air.

IV. Quantitative Correlation of Reaction Stoichiometry, UV-vis Spectra, and XAS Spectra.

Various reactions of **OLE-Ce** were analyzed in parallel by *in situ* XANES and by optical spectroscopy. The molar OD at 340 nm was plotted as a function of the percentage of Ce^{3+} in each sample: blue points in **Figure 3B**, data in Table 1. *For all the **OLE-Ce** samples, there is a linear relationship between the molar OD and the %Ce^{3+}.* This linear correlation extends over a

very wide range of composition, from highly oxidized (13%Ce^{3+}/87%Ce^{4+}) to highly reduced (67%Ce^{3+}/33%Ce^{4+}). The linearity is particularly remarkable because the changes in the %Ce^{3+} have been accomplished in different ways, by photoreduction, chemical reduction, or chemical oxidation with reagents as varied as benzoquinone and ^{t}BuOOH. In addition, all three batches of OLE-Ce follow the same correlation line between the molar absorbance at 340 nm and % Ce^{3+}, even though the as-synthesized materials had significantly different %Ce^{3+} values.

The changes in oxidation state, the x-axis in the correlation, were in many cases measured both by XAS and by NMR integration of the chemical reagents. The same correlations (same slopes within the uncertainties) were observed using the different methods: using direct measurement of % Ce^{3+} by XAS (Figure 3B) and determining the redox change in the ceria NCs (the moles of electrons transferred) by NMR integration (Figure 2C). The close correspondence of the results from NMR, XAS and optical spectroscopy provides strong support for the reproducibility of the results and the conclusions of this study.

A linear correlation was also observed for the **MAA-Ce** samples (red points in Figure 3B; Table 1). Again, higher Ce^{4+} content is characterized by a higher molar absorption. While the same linear correlation is observed, the slope and intercept of the line are different. The value of these correlations is that once the line has been established for a particular batch of nanocrystals, *the optical spectra are a direct and convenient measure of the %Ce^{3+} in the colloidal NCs*. This will be a useful tool for analysis of ceria-based redox processes.

The existence of a linear correlation between optical density and the cerium oxidation state ratio for two quite different types of ceria NCs suggests that this will be a general property. Nevertheless, the correlation line obtained for **MAA-Ce** differs from that of the **OLE-Ce** samples. One possibility is that the capping ligands influence the optical spectra of the material,

which would not be surprising given the large portion of the Ce atoms that are on the surface of these very small NCs (2-3 nm). It is also possible that the correlations depend on the ratio of surface to bulk Ce ions, which was different for **OLE-Ce** (**-a, -b,** and **-c**) and **MAA-Ce** due to their different sizes.

V. Reversibility of the Chemical Processes at Nanoceria. The inner-sphere redox processes of ceria NCs are completely reversible, based on the optical, NMR and XAS assays. For example, photoreduction of **OLE-Ce** followed by BQ oxidation gives essentially the same optical spectrum and Ce^{3+}/Ce^{4+} ratio as reduction by H_2Q (Figure 2A). In one set of experiments, **OLE-Ce** were photo-reduced, then oxidized with TBHP and then reduced again with H_2Q. After each step, the optical spectrum was indicative of changes in oxidation states, while holding the linear relationship (Figure S15, Table S2).

The reversibility – that the linear relationship holds between the optical density at 340 nm and the $\%Ce^{3+}$ in the nanocrystals as the oxidation states are tuned one way and then back – implies that the NCs have not undergone any significant overall changes during cycling. For instance, it is very unlikely that any changes in NC size as a result of the chemical reactions would be reversible. To confirm this, TEM images were obtained for a sample of **OLE-Ce-B** at various redox states: as prepared, reduced with H_2Q, and air oxidized (Figure S17). The average diameters and widths of the distributions were the same within the uncertainty of the measurements: 1.9 ± 0.2 nm; 1.9 ± 0.2 nm, and 2.0 ± 0.3 nm, respectively. The slight growth and broadening were not statistically significant and did not parallel the changes in oxidation state and optical density (down, then up). The reversibility and TEM data show that the changes in

absorption spectra are not due to changes in size. The optical changes reflect the oxidation states, not a quantum confinement effect.

CONCLUSIONS

The experiments above demonstrate the rich redox chemistry of two kinds of colloidal ceria nanocrystals. Under very mild conditions, the percentage of Ce^{3+} has been manipulated from 13% to 67% for the **OLE-Ce** samples, and from 18% to 44% for the **MAA-Ce**. These changes have been accomplished with UV-photoreduction and by treatment with an array of simple organic oxidants and reductants, such as hydroquinone and benzoquinone. Higher Ce^{3+} content results in more reducing NCs. The large changes in average cerium oxidation states imply substantial changes in stoichiometry of the materials, which is likely facilitated by their small size (2-3 nm diameter, ca. 4-6 unit cells across) and the use of reagents that are H-atom or O-atom donors or acceptors, rather than pure electron transfer agents.

The ability to tune the cerium oxidation states up and down has allowed us to demonstrate, for the first time, that the molar optical density of colloidal nanoceria correlate with the $\%Ce^{3+}$ vs. Ce^{4+} in the material. The cerium oxidation states and their changes were measured using x-ray absorption spectroscopy (XAS) and using the stoichiometry of the reactions from ^1H NMR. Results from all three batches of **OLE-Ce** fall on the same correlation line. The **MAA-Ce** samples also show a good linear correlation of molar absorbance vs. average cerium oxidation, though on a different correlation line than the **OLE-Ce** (Figure 3B). We emphasize that this linear correlation was observed between all of the samples of a given type of NC, independent of the type of reagent used to manipulate the redox level of the cerium, and that the optical changes were reversible. This contrasts with prior studies that often assigned optical changes to

transitions involving capping ligands such as catecholates, and that often involved comparisons among different sized nanocrystals. Thus, the decrease in molar absorption originates solely from an increase in Ce^{3+} fraction in ceria NCs (and vice versa), and not due to a quantum size effect. Examining the UV spectra over the whole range from 250 – 400 nm shows that the changes are a bleach of the spectrum, with decreases throughout this range, and not a blue shift of a band edge as previously discussed.

The discovery of a linear correlation of optical density with the percentage of Ce^{3+}, for both lipophilic and hydrophilic ceria nanocrystals and for reactions with a variety of redox agents, is a powerful new tool in the study of nanoceria. A very simple optical measurement can assess reactivity, redox states and properties of potentially any colloidal ceria NC system, with an *in situ*, non-invasive method. We expect that this new tool will prove valuable in many areas of research and application in the rapidly growing field of nanoceria, and we are making much use of it in continuing studies in our own laboratories.

ASSOCIATED CONTENT

Supporting Information. Reactivity and spectroscopic results (PDF). This material is available free of charge via the Internet at http://pubs.acs.org.

AUTHOR INFORMATION

Corresponding Author

*E-mail: james.mayer@yale.edu

Notes

The authors declare no competing financial interest.

ACKNOWLEDGMENT

This work was supported by the U.S. National Science Foundation via NSF CHE-1609434 to JMM and as part of the CCI Center for Enabling New Technologies through Catalysis (CENTC), CHE-1205189. This research used resources of the X-ray Science Division Spectroscopy group (XSD-SPC) at the Advanced Photon Source, a U.S. Department of Energy (DOE) Office of Science User Facility operated for the DOE Office of Science by Argonne National Laboratory under Contract No. DE-AC02-06CH11357.

ABBREVIATIONS

OLE-Ce, oleate-capped cerium oxide; MAA-Ce methoxyacetic acid-capped cerium oxide.

REFERENCES

1. McCabe, R. W.; Trovarelli, A. Forty years of catalysis by ceria: A success story. *Appl. Catal. B: Environ.* **2016,** *197*, 1.

2. Montini, T.; Melchionna, M.; Monai, M.; Fornasiero, P. Fundamentals and Catalytic Applications of CeO_2-Based Materials. *Chem. Rev.* **2016,** *116*, 5987-6041.

3. Trovarelli, A. Catalytic properties of ceria and CeO_2-containing materials. *Catal. Rev.* **1996,** *38*, 439-520.

4. Vivier, L.; Duprez, D. Ceria-Based Solid Catalysts for Organic Chemistry. *ChemSusChem* **2010,** *3*, 654-678.

5. Trovarelli, A., Structural Properties and Nonstoichiometric Behaviour of CeO_2. In *Catalysis by Ceria and Related Materials*, Trovarelli, A., Ed. Imperial College Press 2002; Vol. Volume 2, pp 15-50.

6. Paier, J.; Penschke, C.; Sauer, J. Oxygen Defects and Surface Chemistry of Ceria: Quantum Chemical Studies Compared to Experiment. *Chem. Rev.* **2013,** *113*, 3949-3985.

7. Lamonier, C.; Wrobel, G.; Bonnelle, J. P. Behavior of ceria under hydrogen treatment: thermogravimetry and in situ X-ray diffraction study. *J. Mat. Chem.* **1994,** *4*, 1927.

8. Laachir, A.; Perrichon, V.; Badri, A.; Lamotte, J.; Catherine, E.; Lavalley, J. C.; El Fallah, J.; Hilaire, L.; Le Normand, F.; Quemere, E.; Sauvion, G. N.; Touret, O. Reduction of CeO_2 by hydrogen. Magnetic susceptibility and Fourier-transform infrared, ultraviolet and X-ray photoelectron spectroscopy measurements. *J. Chem. Soc. Faraday Trans.* **1991,** *87*, 1601-1609.

9. Bernal, S.; Calvino, J. J.; Cifredo, G. A.; Gatica, J. M.; Omil, J. A. P.; Pintado, J. M. Hydrogen chemisorption on ceria: influence of the oxide surface area and degree of reduction. *J. Chem. Soc. Faraday Trans.* **1993,** *89*, 3499-3505.

10. Fierro, J. L. G.; Soria, J.; Sanz, J.; Rojo, J. M. Induced changes in ceria by thermal treatments under vacuum or hydrogen. *J. Solid State Chem.* **1987,** *66*, 154-162.

11. Bruce, L. A.; Hoang, M.; Hughes, A. E.; Turney, T. W. Surface area control during the synthesis and reduction of high area ceria catalyst supports. *Appl. Catal. A* **1996,** *134*, 351.

12. Gao, Y.; Li, R.; Chen, S.; Luo, L.; Cao, T.; Huang, W. Morphology-dependent interplay of reduction behaviors, oxygen vacancies and hydroxyl reactivity of CeO_2 nanocrystals. *Phys. Chem. Chem. Phys.* **2015,** *17*, 31862-31871.

13. Wu, X.-P.; Gong, X.-Q. Clustering of Oxygen Vacancies at CeO_2 (111): Critical Role of Hydroxyls. *Phys. Rev. Lett.* **2016,** *116*, 086102.

14. Mogensen, M.; Sammes, N. M.; Tompsett, G. A. Physical, chemical and electrochemical properties of pure and doped ceria. *Solid State Ionics* **2000,** *129*, 63-94.

15. Patsalas, P.; Logothetidis, S.; Sygellou, L.; Kennou, S. Structure-dependent electronic properties of nanocrystalline cerium oxide films. *Phys. Rev. B* **2003,** *68*, 035104.

16. Celardo, I.; Pedersen, J. Z.; Traversa, E.; Ghibelli, L. Pharmacological potential of cerium oxide nanoparticles. *Nanoscale* **2011,** *3*, 1411-1420.

17. Karakoti, A. S.; Monteiro-Riviere, N. A.; Aggarwal, R.; Davis, J. P.; Narayan, R. J.; Self, W. T.; McGinnis, J.; Seal, S. Nanoceria as Antioxidant: Synthesis and Biomedical Applications. *JOM* **2008,** *60*, 33-37.

18. Andreescu, D.; Bulbul, G.; Özel, R. E.; Hayat, A.; Sardesai, N.; Andreescu, S. Applications and implications of nanoceria reactivity: measurement tools and environmental impact. *Environ. Sci. Nano* **2014,** *1*, 445-458.

19. Walkey, C.; Das, S.; Seal, S.; Erlichman, J.; Heckman, K.; Ghibelli, L.; Traversa, E.; McGinnis, J. F.; Self, W. T. Catalytic properties and biomedical applications of cerium oxide nanoparticles. *Environ. Sci. Nano* **2015,** *2*, 33-53.

20. Karakoti, A.; Singh, S.; Dowding, J. M.; Seal, S.; Self, W. T. Redox-active radical scavenging nanomaterials. *Chem. Soc. Rev.* **2010,** *39*, 4422-4432.

21. Ornatska, M.; Sharpe, E.; Andreescu, D.; Andreescu, S. Paper Bioassay Based on Ceria Nanoparticles as Colorimetric Probes. *Anal. Chem.* **2011,** *83*, 4273-4280.

22. Sharpe, E.; Frasco, T.; Andreescu, D.; Andreescu, S. Portable ceria nanoparticle-based assay for rapid detection of food antioxidants (NanoCerac). *The Analyst* **2013,** *138*, 249-262.

23. Bülbül, G.; Hayat, A.; Liu, X.; Andreescu, S. Reactivity of nanoceria particles exposed to biologically relevant catechol-containing molecules. *RSC Advances* **2016,** *6*, 60007-60014.

24. Hayat, A.; Andreescu, D.; Bulbul, G.; Andreescu, S. Redox reactivity of cerium oxide nanoparticles against dopamine. *J. Colloid Interf. Sci.* **2014,** *418*, 240-245.

25. Mitchell, K. J.; Abboud, K. A.; Christou, G. Atomically-precise colloidal nanoparticles of cerium dioxide. *Nature Comm.* **2017,** *8*, 1445.

26. Mathey, L.; Paul, M.; Copéret, C.; Tsurugi, H.; Mashima, K. Cerium(IV) Hexanuclear Clusters from Cerium(III) Precursors: Molecular Models for Oxidative Growth of Ceria Nanoparticles. *Chem. Eur. J.* **2015,** *21*, 13454-13461.

27. Solola, L. A.; Cheisson, T.; Yang, Q.; Carroll, P. J.; Schelter, E. J. Exploration of the Solid- and Solution-State Structures and Electrochemical Properties of Ce^{IV}(atrane) Complexes. *Inorg. Chem.* **2018,** *57*, 10543-10547.

28. Piro, N. A.; Robinson, J. R.; Walsh, P. J.; Schelter, E. J. The electrochemical behavior of cerium(III/IV) complexes: Thermodynamics, kinetics and applications in synthesis. *Coord. Chem. Rev.* **2014,** *260*, 21-36.

29. So, Y.-M.; Leung, W.-H. Recent advances in the coordination chemistry of cerium(IV) complexes. *Coord. Chem. Rev.* **2017,** *340*, 172-197.

30. Williams, U. J.; Mahoney, B. D.; Lewis, A. J.; DeGregorio, P. T.; Carroll, P. J.; Schelter, E. J. Single Crystal to Single Crystal Transformation and Hydrogen-Atom Transfer upon Oxidation of a Cerium Coordination Compound. *Inorg. Chem.* **2013,** *52*, 4142-4144.

31. Baer, D. R.; Engelhard, M. H.; Gaspar, D. J.; Matson, D. W.; Pecher, K. H.; Williams, J. R.; Wang, C. M. Challenges in Applying Surface Analysis Methods to Nanoparticles and Nanostructured Materials. *J. Surf. Anal.* **2005,** *12*, 101-108.

32. Zhang, F.; Wang, P.; Koberstein, J.; Khalid, S.; Chan, S.-W. Cerium oxidation state in ceria nanoparticles studied with X-ray photoelectron spectroscopy and absorption near edge spectroscopy. *Surf. Sci.* **2004,** *563*, 74-82.

33. Wu, L.; Wiesmann, H. J.; Moodenbaugh, A. R.; Klie, R. F.; Zhu, Y.; Welch, D. O.; Suenaga, M. Oxidation state and lattice expansion of CeO_{2-x} nanoparticles as a function of particle size. *Phys. Rev. B* **2004,** *69*, 125415.

34. Wu, T. S.; Zhou, Y.; Sabirianov, R. F.; Mei, W. N.; Soo, Y. L.; Cheung, C. L. X-ray absorption study of ceria nanorods promoting the disproportionation of hydrogen peroxide. *Chem. Comm.* **2016,** *52*, 5003-5006.

35. Martra, G.; Gianotti, E.; Coluccia, S., The Application of UV-Visible-NIR Spectroscopy to Oxides. In *Metal Oxide Catalysis*, Wiley-VCH: 2008; pp 51-94.

36. Tsunekawa, S.; Sivamohan, R.; Ohsuna, T.; Kasuya, A.; Takahashi, H.; Tohji, K. Ultraviolet Absorption Spectra of CeO_2 Nano-Particles. *Mater. Sci. Forum* **1999,** *315–317*, 439.

37. Masui, T.; Fujiwara, K.; Machida, K. i.; Adachi, G. y.; Sakata, T.; Mori, H. Characterization of Cerium(IV) Oxide Ultrafine Particles Prepared Using Reversed Micelles. *Chem. Mater.* **1997,** *9*, 2197.

38. Zhang, F.; Chan, S.-W.; Spanier, J. E.; Apak, E.; Jin, Q.; Robinson, R. D.; Herman, I. P. Cerium oxide nanoparticles: Size-selective formation and structure analysis. *Appl. Phys. Lett.* **2002,** *80*, 127.

39. Tsunekawa, S.; Wang, J.-T.; Kawazoe, Y.; Kasuya, A. Blueshifts in the ultraviolet absorption spectra of cerium oxide nanocrystallites. *J. Appl. Phys.* **2003,** *94*, 3654-3656.

40. Kuchibhatla, S. V.; Karakoti, A. S.; Baer, D. R.; Samudrala, S.; Engelhard, M. H.; Amonette, J. E.; Thevuthasan, S.; Seal, S. Influence of Aging and Environment on Nanoparticle Chemistry - Implication to Confinement Effects in Nanoceria. *J. Phys. Chem. C Nanometer Interf.* **2012,** *116*, 14108-14114.

41. Yin, L. X.; Wang, Y. Q.; Pang, G. S.; Koltypin, Y.; Gedanken, A. Sonochemical synthesis of cerium oxide nanoparticles-effect of additives and quantum size effect. *J. Colloid Interface Sci.* **2002,** *246*, 78.

42. Hernández-Alonso, M. D.; Belén Hungría, A.; Martínez-Arias, A.; Coronado, J. M.; Carlos Conesa, J.; Soria, J.; Fernández-García, M. Confinement effects in quasi-stoichiometric CeO2nanoparticles. *Phys. Chem. Chem. Phys.* **2004,** *6*, 3524-3529.

43. Deshpande, S.; Patil, S.; Kuchibhatla, S. V. N. T.; Seal, S. Size dependency variation in lattice parameter and valency states in nanocrystalline cerium oxide. *Appl. Phys. Lett.* **2005,** *87*, 133113.

44. Tsunekawa, S.; Fukuda, T.; Kasuya, A. X-ray photoelectron spectroscopy of monodisperse CeO2−x nanoparticles. *Surf. Sci.* **2000,** *457*, L437–L440.

45. Reed, K.; Cormack, A.; Kulkarni, A.; Mayton, M.; Sayle, D.; Klaessig, F.; Stadler, B. Exploring the properties and applications of nanoceria: is there still plenty of room at the bottom? *Environ. Sci. Nano* **2014,** *1*, 390-405.

46. Taniguchi, T.; Watanabe, T.; Sakamoto, N.; Matsushita, N.; Yoshimura, M. Aqueous Route to Size-Controlled and Doped Organophilic Ceria Nanocrystals. *Crystal Growth & Design* **2008,** *8*, 3725-3730.

47. *For details see SI.*

48. Lee, S. S.; Song, W.; Cho, M.; Puppala, H. L.; Nguyen, P.; Zhu, H.; Segatori, L.; Colvin, V. L. Antioxidant Properties of Cerium Oxide Nanocrystals as a Function of Nanocrystal Diameter and Surface Coating. *ACS Nano* **2013,** *7*, 9693-9703.

49. Perez, J. M.; Asati, A.; Nath, S.; Kaittanis, C. Synthesis of biocompatible dextran-coated nanoceria with pH-dependent antioxidant properties. *Small* **2008,** *4*, 552-556.

50. Wang, Y. J.; Dong, H.; Lyu, G. M.; Zhang, H. Y.; Ke, J.; Kang, L. Q.; Teng, J. L.; Sun, L. D.; Si, R.; Zhang, J.; Liu, Y. J.; Zhang, Y. W.; Huang, Y. H.; Yan, C. H. Engineering the defect state and reducibility of ceria based nanoparticles for improved anti-oxidation performance. *Nanoscale* **2015,** *7*, 13981-13990.

51. Haase, M.; Weller, H.; Henglein, A. Photochemistry and radiation chemistry of colloidal semiconductors. 23. Electron storage on zinc oxide particles and size quantization. *J. Phys. Chem.* **1988,** *92*, 482-487.

52. Kamat, P. V. Photochemistry on nonreactive and reactive (semiconductor) surfaces. *Chem. Rev.* **1993,** *93*, 267-300.

53. Schrauben, J. N.; Hayoun, R.; Valdez, C. N.; Braten, M.; Fridley, L.; Mayer, J. M. Titanium and zinc oxide nanoparticles are proton-coupled electron transfer agents. *Science* **2012,** *336*, 1298-1301.

54. Warren, J. J.; Tronic, T. A.; Mayer, J. M. Thermochemistry of Proton-Coupled Electron Transfer Reagents and its Implications. *Chem. Rev.* **2010,** *110*, 6961-7001.

55. Nachimuthu, P.; Shih, W.-C.; Liu, R.-S.; Jang, L.-Y.; Chen, J.-M. The Study of Nanocrystalline Cerium Oxide by X-Ray Absorption Spectroscopy. *J. Solid State Chem.* **2000,** *149*, 408-413.

56. Shahin, A. M.; Grandjean, F.; Long, G. J.; Schuman, T. P. Cerium LIII-Edge XAS Investigation of the Structure of Crystalline and Amorphous Cerium Oxides. *Chem. Mat.* **2005,** *17*, 315-321.

57. Bernardi, M. I.; Mesquita, A.; Beron, F.; Pirota, K. R.; de Zevallos, A. O.; Doriguetto, A. C.; de Carvalho, H. B. The role of oxygen vacancies and their location in the magnetic properties of $Ce_{1-x}Cu_xO_{2-\delta}$ nanorods. *Phys. Chem. Chem. Phys.* **2015,** *17*, 3072-3080.

TOC Image

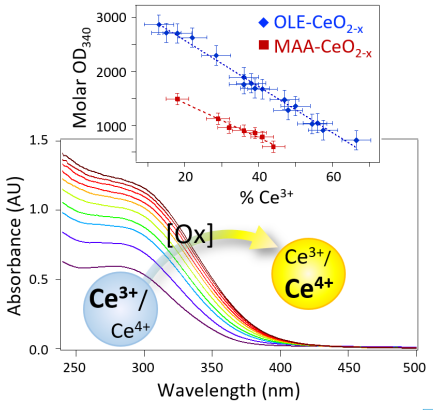

Synopsis

Mild chemical reactions of ceria nanocrystals reversibly tune the Ce^{4+}/Ce^{3+} ratio in the material over a large range, as revealed by stoichiometry and XAS measurements. The optical spectra are observed to linearly correlate with the $\%Ce^{3+}$, providing a powerful new tool for *in situ* determination of Ce oxidation states in these nanocrystals.